Research Square

Preprints are preliminary reports that have not undergone peer review.
They should not be considered conclusive, used to inform clinical practice,
or referenced by the media as validated information.

Hypoxia-Induced HIF-1α Drives the Progression of Odontogenic Keratocysts via the Sonic Hedgehog Pathway and PLK1-Mediated Osteolytic Remodeling

Qixian Gai
Kunming Medical University
Jiabei Mu
Kunming Medical University
Zixian Xu
Kunming Medical University
Yantong Chen
Kunming Medical University
Shan Wang
Kunming Medical University
Zheyi Sun
Kunming Medical University
Jiemei Zhai
zhaijiemei@kmmu.edu.cn

Kunming Medical University

Article

Keywords: Odontogenic Keratocysts, Fibroblasts, HIF-1α, Sonic Hedgehog Signaling Pathway, PLK1

Posted Date: July 1st, 2026

DOI: https://doi.org/10.21203/rs.3.rs-9715763/v1

License: This work is licensed under a Creative Commons Attribution 4.0 International License.
Read Full License

Additional Declarations: No competing interests reported.

Hypoxia-Induced HIF-1α Drives the Progression of Odontogenic Keratocysts via the Sonic Hedgehog Pathway and PLK1-Mediated Osteolytic Remodeling

Qixian Gai[a,b,c†] Jiabei Mu[a†] Zixian Xu[a,b] Yantong Chen[a,b] Shan Wang[a,b]

Zheyi Sun [a,b*] Jiemei Zhai[a,b*]

[a]Kunming Medical University School and Hospital of Stomatology, 1168 Chunrong West Road, Chenggong Zone, Kunming 650500, People's Republic of China. Kunming 650500, People's Republic of China

[b]Yunnan Key Laboratory of Stomatology, 1168 Chunrong West Road, Chenggong Zone, Kunming 650500, People's Republic of China

[c]Department of Stomatology, Luoyang First People's Hospital, Chanjian Avenue, Chanhe Hui District, Luoyang 471000, People's Republic of China.

[*]Corresponding author

Zheyi Sun

Kunming Medical University School and Hospital of Stomatology, 1168 Chunrong West Road, Chenggong Zone, Kunming 650500, People's Republic of China.

Yunnan Key Laboratory of Stomatology, 1168 Chunrong West Road, Chenggong Zone, Kunming 650500, People's Republic of China

E-mail: sunzheyi@kmmu.edu.cn

Jiemei Zhai

Kunming Medical University School and Hospital of Stomatology, 1168 Chunrong West Road, Chenggong Zone, Kunming 650500, People's Republic of China.

Yunnan Key Laboratory of Stomatology, 1168 Chunrong West Road, Chenggong Zone, Kunming 650500, People's Republic of China

Tel: +86-871-65338944

Fax: +86-871-65330116

E-mail: zhaijiemei@kmmu.edu.cn

[†]These authors contributed equally to this work.

Author Contributions

Qixian Gai: Conceptualization, Methodology, Investigation, Formal analysis, Writing – Original Draft.

Jiabei Mu: Conceptualization, Methodology, Investigation, Formal analysis, Writing – Original Draft.

Zixian Xu: Conceptualization, Investigation , Software.

Yantong Chen: Investigation.

Shan Wang: Investigation.

Zheyi Sun: Supervision, Project administration, Funding acquisition, Writing – Review & Editing.

Jiemei Zhai: Conceptualization, Supervision, Funding acquisition, Writing – Review & Editing, Project administration.

Data availability statement

The RNA-seq data generated in this study are not publicly available due to ethical restrictions but are available from the corresponding author (Jiemei Zhai) upon reasonable request. Publicly available datasets analyzed in this study, GSE38494 and GSE176351, are accessible via the NCBI Gene Expression Omnibus (GEO) repository at https://www.ncbi.nlm.nih.gov/geo/.

Funding statement

This work was supported by the National Natural Science Foundation of China (Grant No. 82560195) and the Reserve Talents for Academic and Technical Leaders of Middle-aged and Young People in Yunnan Province (grant number 202305AC160001).

Conflict of interest disclosure

The authors declare that they have no known competing financial interests or personal relationships that could have appeared to influence the work reported in this paper.

Human Ethics Approval

Ethical approval for the human subject involved in this case report was obtained from the Medical Ethics Committee of the Affiliated Stomatological Hospital of Kunming Medical University (Approval Nos. KYKQ2022MEC0074 and KYKQ2024MEC0055). Informed consent was obtained from the patient and/or their legal guardian(s).

Animal Ethics Approval

Ethical approval for the animal study was obtained from the Experimental Animal Welfare Ethics Committee of Kunming Medical University (Approval No. KMMUD2025028). The parts of this study involving human participants were carried out in accordance with the Declaration of Helsinki and relevant guidelines and regulations. All methods were carried out in accordance with relevant guidelines and regulations.

Hypoxia-Induced HIF-1α Drives the Progression of Odontogenic Keratocysts via the Sonic Hedgehog Pathway and PLK1-Mediated Osteolytic Remodeling

Abstract：

Hypoxia drives the progression of odontogenic keratocyst, an aggressive jaw lesion with high recurrence, through a dual mechanism. While mutations in the Sonic Hedgehog signaling pathway are known drivers, the mechanisms in mutation-negative cases remain unclear, and hypoxia within the cyst has been implicated. Using immunohistochemistry, bioinformatics, and in vitro assays with primary odontogenic keratocyst fibroblasts under hypoxic conditions, along with inhibitors targeting hypoxia-inducible factor-1α (HIF-1α) and its effectors, we found that HIF-1α is upregulated in odontogenic keratocyst tissues. Hypoxia activates the Sonic Hedgehog signaling pathway in fibroblasts via HIF-1α, increasing their proliferation and invasion. Furthermore, hypoxia-induced fibroblast secretion upregulates Polo-like kinase 1 in osteoclast precursors, enhancing osteolytic activity. Together, these findings reveal that HIF-1α-mediated Sonic Hedgehog activation promotes fibroblast growth, while hypoxic fibroblasts stimulate osteoclast-mediated bone resorption through Polo-like kinase 1, identifying novel therapeutic targets.

Keywords: Odontogenic Keratocysts; Fibroblasts; HIF-1α; Sonic Hedgehog Signaling Pathway; PLK1

1.INTRODUCTION：

Odontogenic keratocyst (OKC) is a common cystic lesion of the jaws, predominantly occurring as sporadic cases, though it may also be associated with nevoid basal cell carcinoma syndrome (NBCCS)[1,2]. Due to its unique growth pattern and certain tumor-like characteristics, OKC has been the subject of ongoing debate regarding its classification. In the 2005 WHO classification, it was redefined as "keratocystic odontogenic tumor (KCOT)" and categorized as a benign odontogenic tumor, reflecting its neoplastic potential. However, the 2017 WHO classification reverted to the original "odontogenic keratocyst" terminology[3,4]. To date, international consensus on its precise nature remains elusive, with persistent controversy in the academic community[5,6].The current clinical management of OKC primarily relies on surgical intervention. Given its locally aggressive growth pattern, conservative treatments such as enucleation or curettage are associated with high recurrence rates. For large or recurrent OKC, segmental or partial jaw resection is often required, which may lead to significant maxillofacial deformity and functional impairment[7,8]. Therefore, determining how to reduce postoperative recurrence rates and improve patients' quality of life

represents a major challenge in the clinical management of OKC. Elucidating the molecular mechanisms underlying OKC pathogenesis and development, and exploring novel therapeutic strategies, constitute critical scientific questions that urgently need to be addressed in this field.

In recent years, with the deepening understanding of tumor microenvironment (TME) theory, the role of cyst wall-derived fibroblasts in odontogenic keratocyst (OKC) has garnered increasing scientific attention. As pivotal stromal components within the TME, fibroblasts not only establish a bidirectional regulatory network with epithelial cells—driving their aberrant proliferative and invasive phenotypes — but also contribute to disease progression by remodeling Extracellular Matrix（ECM） architecture, recruiting immune cells, and promoting angiogenesis[9,10,11]. In OKC, the interaction between cyst wall fibroblasts and the epithelial lining forms a unique pathogenic microenvironment.

Hypoxia represents a critical feature of the TME[12,13,14].Hypoxia inducible factors (HIFs) are pivotal transcriptional regulators enabling tumor cell adaptation to hypoxic microenvironments[15]. HIF-1α, the principal oxygen-regulated transcriptional factor within the HIF family, is recognized as a critical biomarker of hypoxic niches[16]. HIF-1α drives tumor proliferation, invasion, and metastasis, while also modulating skeletal homeostasis through bidirectional regulation of osteogenic and osteoclastic activities[17,18,19,20,21,22]. Emerging evidence suggests potential hypoxia within the microenvironment of OKC. Therefore, elucidating the hypoxic status in OKC has become an imperative task for unraveling the root cause of its aggressive biological behavior, calling for in-depth investigation.

Previous studies have demonstrated that PTCH1 gene mutations in the OKC lining epithelium lead to aberrant activation of the SHH signaling pathway, thereby driving disease progression[23,24]. However, recent evidence indicates that PTCH1 mutations are absent in a subset of OKC epithelial samples, suggesting the involvement of novel molecular mechanisms in the pathogenesis and progression of OKC[25].

Previous studies have demonstrated that aberrant activation of the Sonic Hedgehog (SHH) pathway during tumorigenesis is associated with hypoxia-mediated HIF-1α. Mian Wei et al. revealed that hypoxic microenvironments in gliomas upregulate HIF-1α, promoting SHH ligand autocrine secretion[26]. This process relieves *PTCH1*-mediated suppression of *SMO*, drives *GLI1* nuclear translocation, and activates the SHH pathway in tumor cells via a ligand-dependent autocrine mechanism. Jianjun Lei et al. further demonstrated that under hypoxic conditions in pancreatic cancer, HIF-1α induces epithelial-mesenchymal transition (EMT) and enhances invasive potential through ligand-independent SHH signaling[27]. These findings collectively highlight the critical role of HIF-1α in modulating SHH pathway activity under hypoxia. Therefore, the precise role and mechanism of the hypoxia-HIF-1α axis in

OKC require investigation.

In this study, we detected the hypoxia-related marker HIF-1α in OKC tissue specimens and confirmed that HIF-1α promotes the proliferation and invasion of OKC fibroblasts by activating the SHH signaling pathway. Subsequent single-cell bioinformatics analysis suggested a potential close association between HIF-1α and osteogenesis or osteoclastogenesis in OKC. Interestingly, however, cellular experiments did not support the notion that HIF-1α alters osteogenic or osteoclastic activity via the SHH pathway. Further bioinformatics analysis and in vitro experiments collectively demonstrate that hypoxia promotes bone remodeling in the microenvironment primarily by regulating OKC fibroblasts through PLK1. These investigations aim to provide experimental evidence for elucidating the pathogenesis of OKC and advancing preventive or therapeutic strategies.

2. MATERIALS AND METHODS

2.1 Patients and samples

This study was approved by the Medical Ethics Committee of the Affiliated Stomatological Hospital of Kunming Medical University (Approval Nos. KYKQ2022MEC0074 and KYKQ2024MEC0055) and the Experimental Animal Welfare Ethics Committee of Kunming Medical University(Approval Nos. KMMUD2025028. The parts of this study involving human participants were carried out in accordance with the Declaration of Helsinki and relevant guidelines and regulations. All methods were carried out in accordance with relevant guidelines and regulations. Paraffin-embedded specimens from 30 sporadic odontogenic keratocyst (OKC) cases and 8 dentigerous cyst (DC) controls were collected from archived samples (2018–2022). Fresh OKC tissues (n=8, pathologically confirmed postoperatively) and control normal oral mucosa (OM) tissues (n=8, obtained from residual mucosal fragments following impacted tooth extraction) were also acquired. A subset of tissues was processed for paraffin sectioning, while the remaining tissues were used for primary fibroblast isolation via the tissue explant method. Cells within passage 5 (P5) were employed in subsequent experiments to ensure phenotypic stability.

Thirty SD rats and thirty C57 mice were procured from the university's Experimental Animal Department and utilized as required by the experimental protocol. All animals were euthanized via cervical dislocation under anesthesia. Mice and rats received an intraperitoneal overdose of 2% pentobarbital sodium at 0.075 mL/10 g body weight (150 mg/kg). Cessation of heartbeat and respiration confirmed death, with cervical dislocation as a secondary method. All procedures followed the AVMA Guidelines for the Euthanasia of Animals. Primary rat bone marrow mesenchymal stem cells (rBMSCs) and mouse bone marrow-derived macrophages (mBMMs) were then isolated using a bone marrow flushing method from the femora and tibiae. The specific procedures were as follows: Femora and tibiae were

aseptically dissected from 3-week-old rats or mice, cleaned with PBS containing antibiotics, and their ends were cut off. The bone marrow cavities were flushed with complete medium to obtain cell suspensions. For rBMSCs, the pelleted cells after centrifugation were directly resuspended and cultured. For mBMMs, the cell pellet was treated with red blood cell lysis buffer, resuspended, and pre-cultured. After 24 hours, non-adherent cells were collected, counted, and seeded at a density of 5×10^4 cells/cm² to obtain purified mBMMs. All cells were cultured at 37°C under 5% CO_2.

2.2 Bioinformatics analysis

This study analyzed transcriptomic data from the NCBI GEO dataset GSE38494 (11 OKC tissues vs. 4 normal oral mucosa samples) using RStudio (v4.3.1) and the limma package (v3.58.1) to identify differentially expressed genes (DEGs) with thresholds set at $|log2FC| > 1.0$ and FDR-adjusted p-value < 0.05. Subsequent Gene Ontology (GO) biological process enrichment analysis was performed with the ClusterProfiler package (v4.10.1). Single-sample Gene Set Enrichment Analysis (ssGSEA) via the GSVA package (v1.50.5) was employed to evaluate cell type-characteristic functional activity, while Gene Set Enrichment Analysis (GSEA) assessed hypoxia pathway and Hedgehog signaling activity. For single-cell RNA sequencing data (GSE176351, 3 OKC specimens), Seurat (v5.2.1) was employed for standardized processing: cells were retained after quality control (nFeature_RNA > 200 and mitochondrial gene percentage < 10%), followed by log-normalization and selection of 2,000 highly variable genes. Data integration across samples was achieved through canonical correlation analysis (CCA), with UMAP dimensionality reduction and Louvain clustering (resolution = 0.6) applied to construct a single-cell atlas. Cell subpopulations were annotated based on marker genes from the CellMarker 2.0 database. Gene expression analysis was performed to identify spatial expression patterns. Patterns of hypoxia-, proliferation-, invasion-, and bone remodeling-related genes were mapped across cellular clusters.

2.3 Immunohistochemistry & Semi-Quantitative Analysis

Five 20× microscopic fields from both the epithelial and stromal regions of each specimen were analyzed. Mean optical density (IOD/AREA) was quantified using ImageJ software (v1.52). Spearman's rank correlation analysis was performed with GraphPad Prism (v5.03), with statistical significance set at $P < 0.05$.

2.4 Primary culture of OKC fibroblasts

Fresh post-operative OKC tissues were immediately rinsed five times with HBSS buffer (Gibco) containing 10% penicillin-streptomycin (Gibco, Waltham, MA, USA), minced with sterile ophthalmic scissors, and cultured in DMEM/F12 medium (Vivacell, Shanghai, China) supplemented with 1% penicillin-streptomycin and 10% fetal bovine serum (FBS, ExCell,

Suzhou, China). Cells were maintained at 37°C in a 5% CO_2 incubator. The complete medium was replaced every 3–5 days. Cells within P5 were used for experiments to ensure phenotypic stability.

2.5 Hypoxic Culture of OKC Fibroblasts

The Billups-Rothenberg hypoxic culture chamber was utilized to simulate a low-oxygen environment. After cell adhesion, the cells were transferred into the chamber and infused with a gas mixture of 94% N_2/5% CO_2 until the oxygen concentration stabilized at 1%. The chamber was then transferred to a standard 37°C, 5% CO_2 incubator for hypoxia treatment. All procedures were maintained throughout the entire experimental process within the sealed hypoxic environment (1% O_2) to prevent reoxygenation.

2.6 CCK8 assay

Cells were seeded in 96-well plates at a density of 1×10^4 cells/well. After 24 hours, graded concentrations of KC7F2 were added. The plates were transferred to a hypoxic chamber (1% O_2) for 24-hour hypoxia treatment, with the normoxic control group maintained in a standard incubator. Following hypoxia exposure, 10 μL of CCK-8 reagent was added to each well, followed by an additional 2-hour incubation under hypoxic conditions. Absorbance at 450nm was measured using a microplate reader.

2.7 Western blot

Total protein lysates (10 μg per lane) were separated by 10% SDS-polyacrylamide gel electrophoresis (SDS-PAGE) and transferred onto polyvinylidene fluoride (PVDF) membranes. Primary antibodies included hypoxia markers (HIF-1α, Abcam, Cambridge, UK), Hedgehog signaling markers (SHH and GLI1, Abcam, Cambridge, UK), bone remodeling markers (RUNX2, BMP4, CTSK, and MMP9, Abcam, Cambridge, UK), and the loading control β-actin (Huaxingbio, Beijing, China). Membranes were incubated with goat anti-rabbit or anti-mouse secondary antibodies (Huaxingbio, Beijing, China), and protein bands were visualized using the Omni-ECL™ Ultrasensitive Chemiluminescence Detection Kit (Epizyme, Shanghai, China). All markers cropped from different parts of the same gel (see Supplementary 1 Information).

2.8 5-Ethynyl-20-deoxyuridine (EdU) assay

OKC fibroblasts were seeded in 48-well plates (2×10^4 cells/well) and labeled with 50μM EdU in complete medium for 2 h. Cells were washed with PBS, fixed in 4% paraformaldehyde (30 min, RT), treated with 2 mg/mL glycine (5 min), and permeabilized with 0.5% Triton X-100 (10 min). Apollo® staining (100 μL/well, 30 min, dark) was followed by methanol rinses and Hoechst 33342 nuclear counterstaining (30 min, dark). After PBS washes, EdU incorporation (red) and nuclei (blue) were imaged via fluorescence microscopy.

Proliferation rates were quantified as EdU^+/total nuclei ratios using ImageJ.

2.9 Transwell invasion assay

Transwell inserts were coated on the upper chamber surface with 50 mg/L Matrigel (1:8 dilution), air-dried at 4°C, and rehydrated with 10 g/L BSA-supplemented serum-free medium for 30 min. Serum-starved cells (12 h) were digested, resuspended in serum-free medium at 2×10^5 cells/mL, and 200 μL of the suspension was added to the upper chamber. The lower chamber received 500 μL of medium containing 15% FBS, with bubble-free placement ensured. After 24 h hypoxia (1% O_2), migrated cells on the lower membrane surface were fixed with 70% methanol (30 min), stained with 0.1% crystal violet, and quantified by averaging cell counts from three randomly selected microscopic fields.

2.10 Primary culture of rat bone marrow mesenchymal stem cells (rBMSCs) and mouse bone marrow-derived macrophages (mBMMs)

Three-week-old specific pathogen-free (SPF) Sprague-Dawley rats and C57 mice were euthanized and subjected to surface disinfection. Bilateral femurs and tibias were aseptically excised, and rat bone marrow-derived mesenchymal stem cells (rBMSCs) and mouse bone marrow mononuclear macrophages (mBMMs) were isolated under sterile conditions. Among them, rBMSCs were used for osteogenic induction experiments, while mBMMs were used for osteoclastic induction experiments.

2.11 Conditioned Medium (CM) Preparation and Application

OKC and OM fibroblasts were serially passaged (P0–P4, without cryopreservation) and cultured to 80% confluency. The original medium was discarded, followed by five PBS washes and replacement with unsupplemented α-MEM basal medium (Gibco, Waltham, MA, USA). After 24 hours, cell supernatants were collected (supernatants from the HYPO-OKC group were subjected to hypoxic treatment as described in section 2.5, while the OKC group and OM group were maintained under standard culture conditions) and stored at −80°C for subsequent use. For follow-up experiments, the collected supernatants were mixed with fresh α-MEM at a 1:3 ratio, supplemented with 10% FBS and 1% penicillin-streptomycin, to prepare conditioned medium (CM) for culturing rBMSCs and mBMMs. All media were prepared immediately before use to avoid growth factor degradation. The final bone remodeling-related experiments were divided into four groups: (1) NC group: rBMSCs or mBMMs cultured without any CM; (2) OM group: rBMSCs or mBMMs cultured with CM derived from OM fibroblasts; (3) OKC group: rBMSCs or mBMMs cultured with CM derived from OKC fibroblasts cultured under normoxic conditions; (4) HYPO-OKC group: rBMSCs or mBMMs cultured with CM derived from OKC fibroblasts cultured under hypoxic conditions.

2.12 Alkaline Phosphatase (ALP) Staining and activity assay

ALP staining: Following PBS washes and 4% paraformaldehyde fixation, cells were incubated with freshly prepared BCIP/NBT chromogenic solution (3 mL alkaline phosphatase buffer, 10 μL BCIP, 20 μL NBT) under dark conditions for 15 ± 2 min until purple-blue precipitates formed. Reactions were terminated with distilled water, and grayscale values were quantified using ImageJ.

ALP activity assay: Cells were lysed (80 μL lysis buffer, 15 min ice bath, sonication, 12,000 rpm centrifugation), and supernatants were incubated with chilled substrate and a pNPP standard gradient (4–40 μL of 0.5 mM) at 37°C for 10 min. Absorbance at 405 nm was measured, and ALP activity (U/L) was calculated via four-parameter logistic regression based on standard curves.

2.13 TRAP-Positive Staining and Bone Resorption Pit Assay

TRAP-positive staining: Cells were washed with PBS, fixed in 4% paraformaldehyde (4°C, 10 min), and incubated with TRAP staining solution (37°C, 4 h, dark) to develop purple-red precipitates. Nuclei were counterstained with hematoxylin (0.1%, 3 min), and TRAP-positive area density was quantified using ImageJ.

Bone resorption pit assay: ethanol-sterilized bovine bone slices were seeded with cells (1×10^4/well). After 10 days of culture, cells were removed, and resorption pit morphology was examined under SEM (200× magnification). Resorption area was quantified via ImageJ.

2.14 RNA isolation and quantitative real-time PCR analysis

Total RNA was isolated using the SteadyPure Rapid RNA Extraction Kit (AG Aikerui, Changsha, Hunan, China), and cDNA was synthesized with the Evo M-MLV Reverse Transcription Premix Kit (AG Aikerui, Changsha, Hunan, China). Quantitative real-time PCR (qPCR) was performed in a final reaction volume of 20 μL using the SYBR Green® Premixed qPCR Kit (AG Aikerui, Changsha, Hunan, China).

We used the primers for Bmp2、Ctsk、Mmp9、Nfatc1、Actb-r、Actb-m, and analyzed the relative expression of individual genes using the $2^{-\Delta\Delta Ct}$ method normalized to β-actin.

Table1 Primer sequences for real-time quantitative PCR

Gene	Forward sequence	Reverse sequence
Bmp2	AACACCGTGCTCAGCTTCCATC	CGAAAAATCTGGAGCTCTGCAG
Ctsk	CTTCCAATACGTGCAGCAGA	TCTTCAGGGCTT TCTCGTTC
Mmp9	GCAGAGGCATACTTGTACCG	TGATGTTATGATGGTCCCACTTG

Nfatc1	GACCCGGAGTTCGACTTCG	TGACACTAGGGGACACATAACTG
Actb-r	CTACCTCATGAAGATCCTGACC	CACAGCTTCTCTTTGATGTCAC
Actb-m	GCTGTATTCCCCTCCATCGTG	CACGGTTGGCCTTAGGGTTCAG

2.15 Pharmacological intervention experiments

For KC7F2 and GANT-61 inhibitor studies, control groups (hypoxia + vehicle: DMSO or ethanol) and experimental groups (hypoxia + 20μM KC7F2 or 10μM GANT-61) were established. OKC fibroblasts were seeded in plates for 24h, followed by media replacement with corresponding inhibitors or equal-volume normal control medium (10% DMEM-F12). Hypoxic treatment (1% O_2) was applied for 24h before downstream assays.

For the nMS-1286937 inhibitor study, the following groups were established:(1) NC group: mBMMs cultured in medium without any CM or nMS-1286937; (2) NC+DMSO group: mBMMs cultured in medium without any CM but containing the same amount of DMSO vehicle as the treatment group; (3) HYPO-OKC+DMSO group: mBMMs cultured in medium containing CM derived from OKC fibroblasts cultured under hypoxic conditions and the same amount of DMSO vehicle as the treatment group; (4) HYPO-OKC+inhibitor group: mBMMs cultured in medium containing CM derived from OKC fibroblasts cultured under hypoxic conditions and nMS-1286937.

2.16 Shh ELISA kit assay

Following 24-hour treatment with 20 μM HIF-1α inhibitor KC7F2 under hypoxic conditions (1% O_2), cell supernatants were collected. Sonic hedgehog (Shh) levels in the supernatants were quantified using a Shh ELISA kit (Enzyme-linked Biotechnology, Shanghai, China).

2.17 Sequencing Sample Preparation:

Samples for sequencing were prepared from mBMMs cultured with CM derived from OKC fibroblasts under normoxic or hypoxic conditions when multinucleated cells became prominent (day 7). Briefly, the culture medium was removed, and the cells were washed twice with 500 μL of nuclease-free PBS at room temperature, incubating for 1 minute per wash. After completely aspirating the PBS, 1 mL of TRIzol reagent was added to each well, and the cells were repeatedly pipetted until complete lysis was achieved, indicated by a non-viscous, clear solution. The entire lysate was then transferred to a conical tube, rapidly frozen in liquid

nitrogen, and stored at −80°C prior to dry ice shipment. mRNA transcriptome sequencing was performed by Shanghai Jialu Biotechnology Center.

2.18 Statistical analysis

Data are expressed as mean ± SD. Analyses and graphs were generated using GraphPad Prism. Group comparisons used unpaired t-tests (two groups) or one-way ANOVA (multiple groups), with FDR-adjusted *P*-values (⩽5%). Values were considered statistically significant at $P < 0.05$, and all experiments were performed three times.

3. RESULTS

3.1 Analysis of OKC tissue transcriptome sequencing data

To investigate the potential association between the clinical phenotypes of OKC and their gene expression features, we first analyzed the GEO dataset GSE38494 (containing mRNA microarray data from 12 OKC cases and 4 normal oral tissue samples). Compared to normal oral mucosal (OM) tissues, OKC tissues exhibited significant enrichment of biological processes related to hypoxia, proliferation, and bone remodeling (Figure 1 b). The characteristic functional activities of "osteoblast" and "osteoclast" cell types in OKC were markedly higher than those in OM (Figure 1 c,d). Additionally, hypoxia-related pathways and the Hedgehog signaling pathway were robustly activated in OKC (Figure 1 e,f).

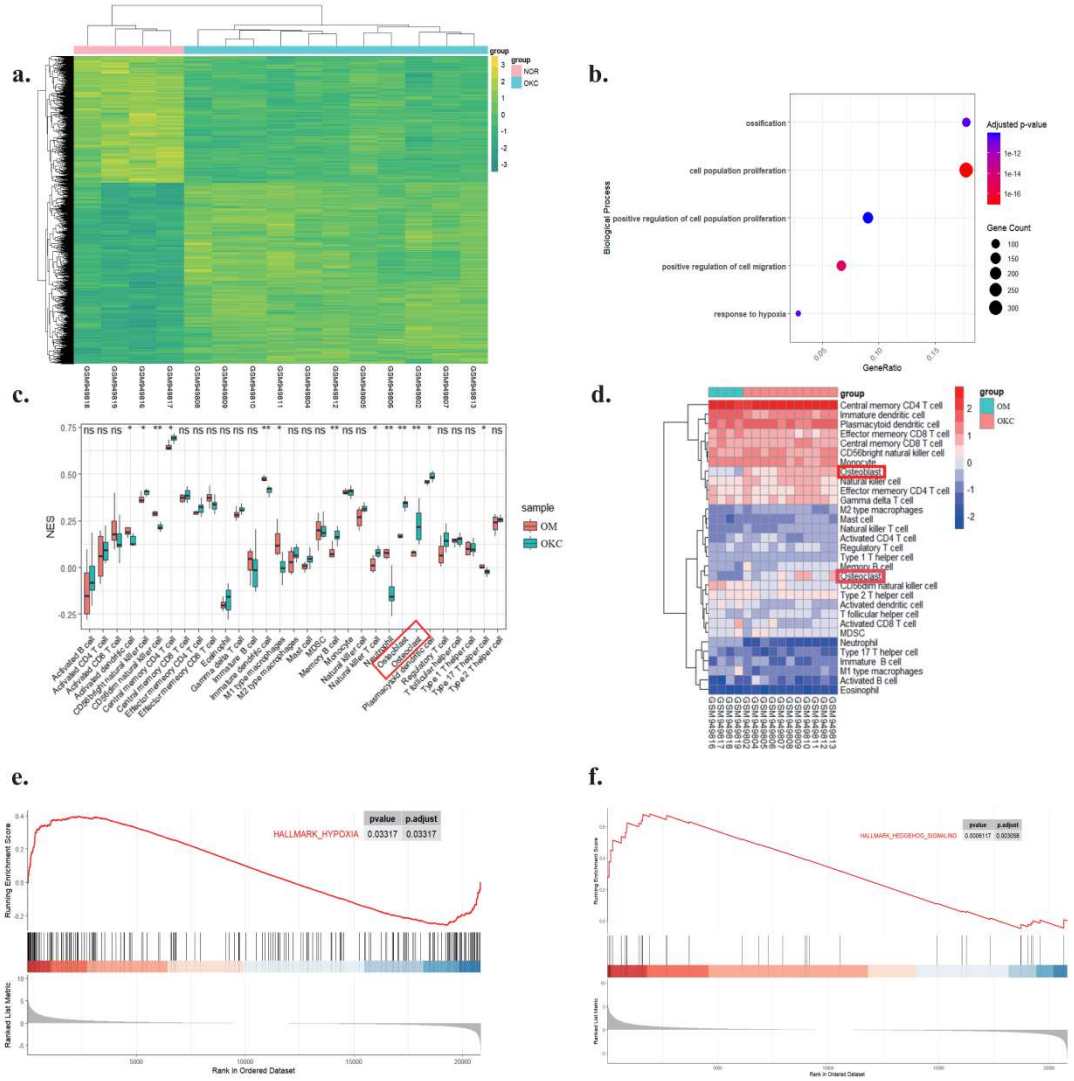


FIGURE 1 (a) Heatmap of differential expression analysis; (b) GO enrichment analysis identified significantly enriched biological processes in OKC tissues compared to OM tissues;(c) Boxplot of ssGSEA;(d) Heatmap of ssGSEA;(e) GSEA detected the overall enrichment trends of hypoxia-related gene sets in OKC tissues; (f) GSEA detected the overall enrichment trends of Hedgehog (HH) signaling pathway-related gene sets in OKC tissues.($^{ns}P \geq 0.05$, $^{*}P < 0.05$, $^{**}P < 0.01$, $^{***}P < 0.001$)

3.2 single-cell transcriptome sequencing data

We analyzed the single-cell RNA sequencing dataset GSE176351 from the GEO database, which includes 3 OKC samples. Integrated data underwent UMAP dimensionality reduction and clustering. Differential gene expression analysis and annotation of major cell populations was performed. Characteristic cell clusters present in OKC included fibroblasts, epithelial cells, and endothelial cells, among others (Figure 2a). Results of Gene expression spatial mapping analysis demonstrate that markers associated with hypoxia, proliferation, and invasion were relatively uniformly localized across the various cell clusters (including

fibroblasts, epithelial cells, endothelial cells, etc.); In contrast, markers related to bone remodeling were preferentially localized within the fibroblast cluster(Figures 2b-d).

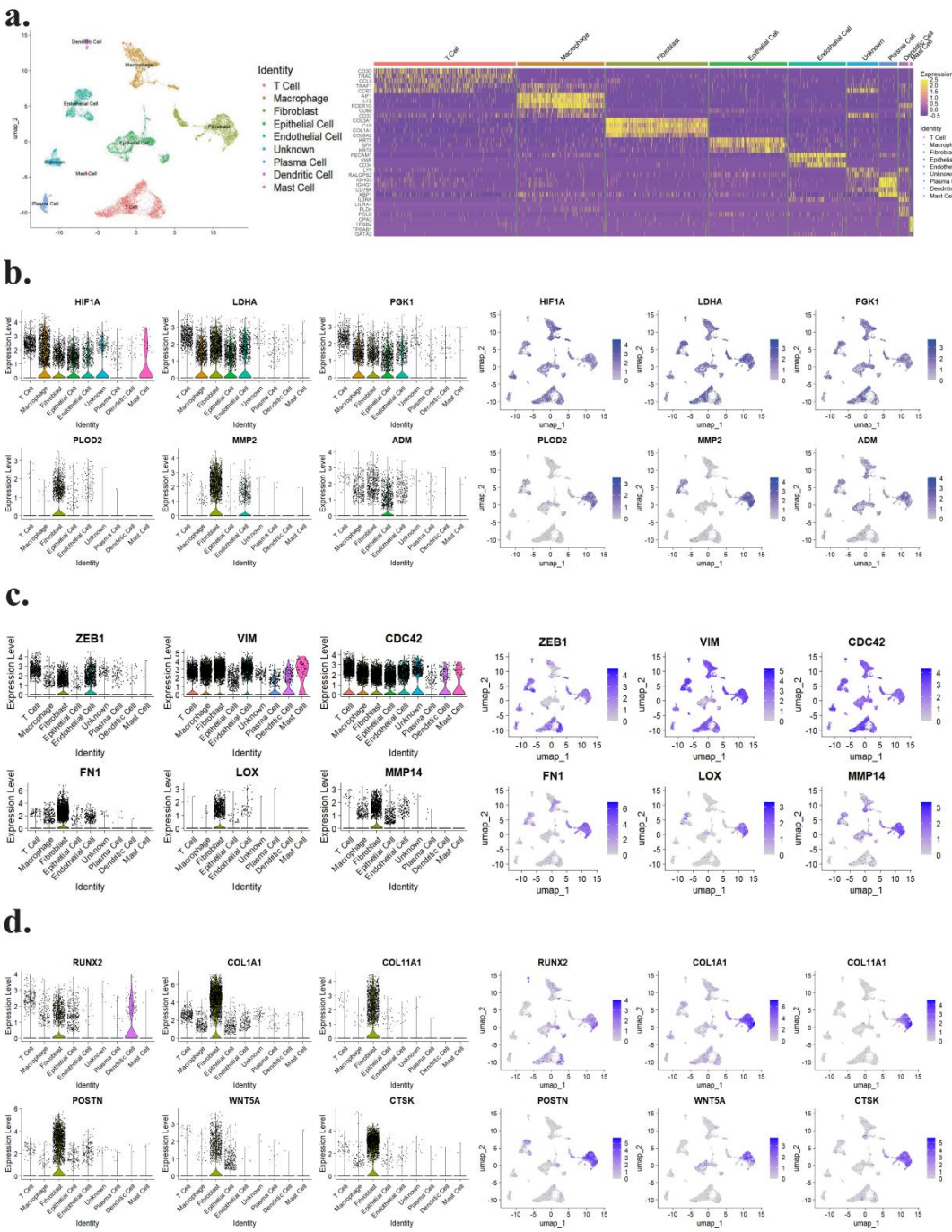


FIGURE 2 (a) Plot results of UMAP clustering and cell type annotation and Heatmap of Differential Marker Gene Expression Across Cell Clusters; (b) Expression Distribution of Genes Related to Hypoxia; (c) Expression Distribution of Genes Related to Proliferation, Invasion, and Migration; (d) Expression Distribution of Genes Related to Bone Remodeling.

3.3 HIF-1α, GLI1, Ki-67, and MMP-9 expression was significantly upregulated in OKC stroma compared to OM and DC controls (IHC).

Immunohistochemical analysis demonstrated significant upregulation of hypoxia marker HIF-1α, SHH signaling effector GLI1, proliferation marker Ki-67, and invasion marker MMP-9 in both epithelial and stromal compartments of OKC compared to oral mucosal (OM) and dentigerous cyst (DC) controls (Figure3a,b,f,g). Spearman's rank correlation analysis demonstrated significant positive correlations between HIF-1α expression and GLI1, Ki-67, and MMP-9 (Figures 3c-e,h-j).

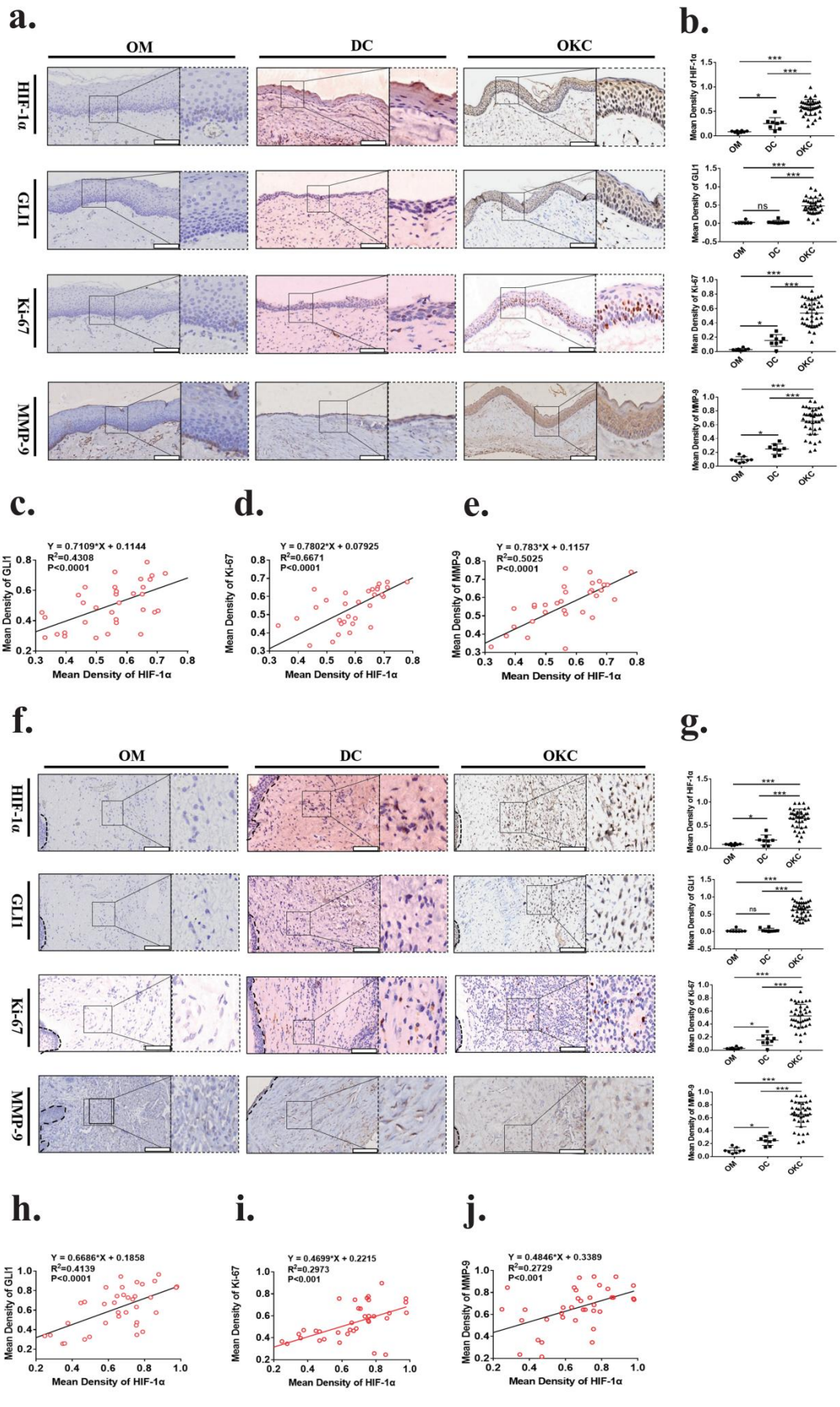


FIGURE 3 (a) The expression of HIF-1α, GLI1, Ki-67, and MMP-9 in the epithelium of

OKC tissues. Scale bar =100μm;(b) Quantitative analysis of HIF-1α, GLI1, Ki-67, and MMP-9 expression levels in the epithelium of OKC tissues;(c) Correlation analysis between HIF-1α and GLI1 expression in the epithelium of OKC tissues; (d) Correlation analysis between HIF-1α and Ki-67 expression in the epithelium of OKC tissues;(e) Correlation analysis between HIF-1α and MMP9 expression in the epithelium of OKC tissues;(f) Expression of HIF-1α, GLI1, Ki-67, and MMP-9 in the stroma of OKC tissues. Scale bar = 100 μm; (g) Quantitative analysis of HIF-1α, GLI1, Ki-67, and MMP-9 expression levels in the stroma of OKC tissues;(h) Correlation analysis between HIF-1α and GLI1 expression in the stroma of OKC tissues;(i) Correlation analysis between HIF-1α and Ki-67 expression in the stroma of OKC tissues;(j) Correlation analysis between HIF-1α and MMP9 expression in the stroma of OKC tissues.($^{ns}P \geq 0.05$, $^{*}P < 0.05$, $^{**}P < 0.01$, $^{***}P < 0.001$)

3.4 Hypoxia-mediated HIF-1α promotes proliferation and invasive potential of OKC fibroblasts.

In OKC fibroblasts, Western Blot analysis was employed to detect HIF-1α expression. Under hypoxic conditions , HIF-1α expression was consistently elevated, peaking at 24h with preserved cell viability. Therefore, subsequent experiments utilized 24h hypoxia (Figure 4a-c). KC7F2, a HIF-1α inhibitor, suppresses HIF-1α expression by blocking HIF-1α protein synthesis. In this experiment, under hypoxic conditions, OKC fibroblasts were treated with different concentrations of KC7F2 for 24h. Cell morphology was then observed microscopically, and cell viability was assessed using the CCK8 assay kit. Following treatment with 20μM KC7F2 for 24h, OKC fibroblasts exhibited well-maintained morphology under microscopic observation. However, treatment with 30 μM KC7F2 for 24h resulted in observable partial cell death(Figure 4d).CCK8 assay results indicated that concentrations of KC7F2 (5μM-20μM) had no significant effect on cell viability. Based on the CCK8 results, 20μM KC7F2 was selected for all subsequent experiments (Figure 4e).Western blot analysis revealed that in OKC fibroblasts, HIF-1α expression was significantly elevated in the Hypoxia group compared to the Normoxia group. No significant difference in HIF-1α expression was observed between the Hypoxia group and the Hypoxia + DMSO control group. However, the Hypoxia+KC7F2 (20μM) group exhibited significantly reduced HIF-1α expression relative to the Hypoxia+DMSO group. These results collectively demonstrate that 24-hour treatment with the HIF-1α inhibitor KC7F2 (20μM) effectively suppresses hypoxia-induced HIF-1α expression in OKC fibroblasts under in vitro conditions (Figure 4f,g). EdU proliferation assays demonstrated that hypoxia significantly increased EdU^{+} cell rates compared to normoxia, while hypoxia+DMSO showed no difference from hypoxia alone(Figure 4h,i). Notably, HIF-1α inhibition with KC7F2 (20 μM) markedly suppressed hypoxia-induced proliferation. Similarly, Transwell invasion assays revealed hypoxia-enhanced Matrigel invasion, unaffected by DMSO but significantly attenuated by

KC7F2(Figure 4j,k). These results indicate that hypoxia promotes OKC fibroblast proliferation and invasion via HIF-1α, both reversible by KC7F2 .

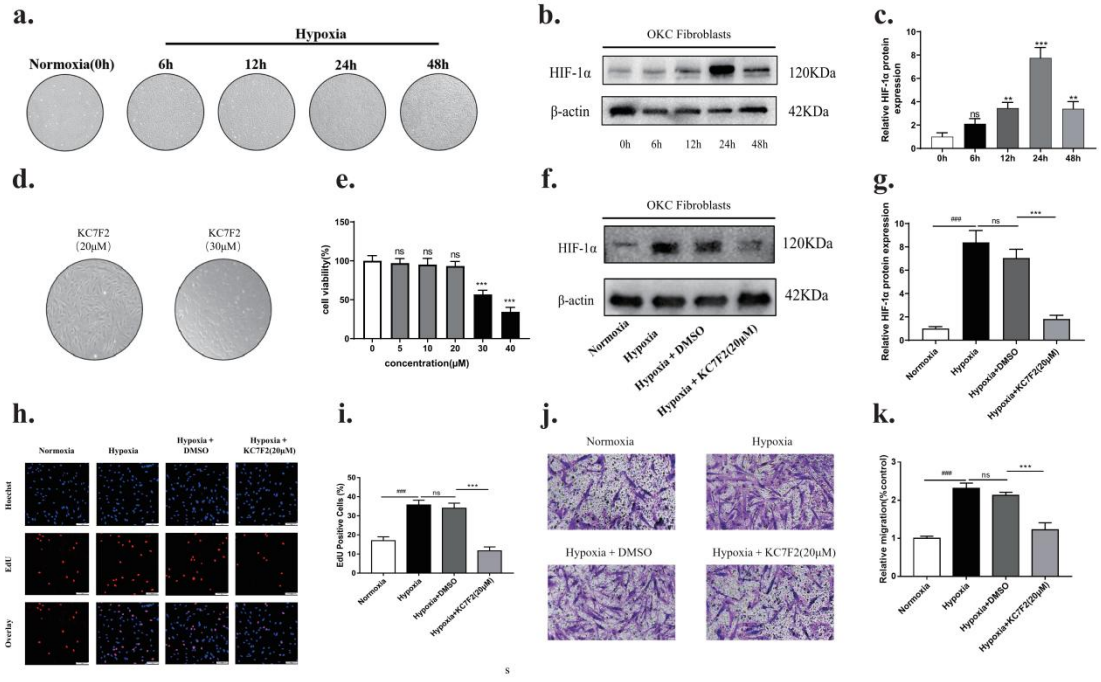


FIGURE 4 (a) Proliferation of OKC fibroblasts under in vitro hypoxic conditions at different time points (10×);(b) Western Blot analysis of HIF-1α expression in OKC fibroblasts following hypoxia treatment (1% O_2); (c) Quantitative analysis of HIF-1α expression in OKC; (d) Under hypoxic conditions, OKC fibroblasts were treated with 20 μM and 30 μM KC7F2 for 24 hours, followed by microscopic examination of cellular growth status (20×);(e) The CCK-8 assay was performed to assess cell viability under hypoxic conditions after 24-hour treatment with graded concentrations of KC7F2;(f) HIF-1α protein expression levels in OKC fibroblasts; (g) Statistical analysis of HIF-1α protein expression in OKC fibroblasts; (h) EdU labeling in OKC primary fibroblasts treated with the HIF-1α inhibitor KC7F2 for 24 hours was observed under fluorescence microscopy;(i) Quantitative analysis of EdU-positive cell percentage in OKC: Blue fluorescence (DAPI-stained nuclei) and red fluorescence (EdU-labeled proliferating cells); (j) Cell invasion through Matrigel-coated chambers in OKC fibroblasts treated with the HIF-1α inhibitor KC7F2 for 24 hours; (k) Quantitative analysis of cell invasion through Matrigel-coated chambers in OKC fibroblasts.($^{ns}P \geq 0.05$, $^{*}P < 0.05$, $^{**}P < 0.01$, $^{***}P < 0.001$) .

3.5 Hypoxia-mediated HIF-1α enhances extracellular Shh secretion and upregulates SHH pathway molecules (SHH, GLI1) in OKC fibroblasts, effects reversed by KC7F2.

ELISA quantification of Shh secretion revealed significantly elevated Shh levels in supernatants of OKC fibroblasts under Hypoxia versus Normoxia . Hypoxia+DMSO controls

showed no significant difference in Shh secretion compared to Hypoxia alone, confirming DMSO's inertness. Furthermore, pharmacological inhibition of HIF-1α with 20 μM KC7F2 (Hypoxia+KC7F2 20μM) significantly suppressed Shh secretion relative to Hypoxia+DMSO (Figure 5a). Following 24-hour treatment with the HIF-1α inhibitor KC7F2, cells were harvested for total protein extraction. Western Blot analysis was performed to detect expression of SHH pathway key molecules (SHH, GLI1). In OKC fibroblasts, SHH and GLI1 expression were significantly elevated in the Hypoxia group compared to Normoxia;No significant difference was observed between the Hypoxia and Hypoxia + DMSO groups.The Hypoxia + KC7F2 (20 μM) group exhibited significantly reduced SHH/GLI1 expression versus Hypoxia + DMSO (Figure 5b-d). Collectively with ELISA data, these results demonstrate that hypoxia-mediated HIF-1α activates the SHH signaling pathway in OKC fibroblasts.

3.6 GANT-61, a GLI1 inhibitor, suppresses hypoxia-induced proliferation and invasion of OKC fibroblasts.

In OKC fibroblasts, Western blot analysis revealed (Figure 5e,f) that treatment with the GLI1 inhibitor GANT-61 (10μM) under hypoxic conditions for 24 hours significantly reduced GLI1 protein expression compared to the hypoxia + ethanol solvent group (Hypoxia+Ethanol), with the GANT-61 concentration determined by previous studies from our research group; HIF-1α expression levels remained unchanged (Figure 5g), indicating that hypoxia activates the SHH pathway via HIF-1α, with HIF-1α acting upstream of SHH signaling. EdU proliferation assays further demonstrated a marked decrease in EdU-positive cell rates in the hypoxia + GANT-61 group (Hypoxia+GANT-61 10 μM) compared to the hypoxia + ethanol group (Figure 5h,i), suggesting that GLI1 inhibition reduces proliferative activity of OKC fibroblasts under hypoxic conditions. Further Transwell invasion assays demonstrated that Hypoxia + GANT-61 (10 μM)-treated OKC fibroblasts exhibited significantly reduced migration through Matrigel-coated chambers compared to the Hypoxia+Ethanol solvent control group(Figure 5j, k). These results indicate that pharmacological inhibition of GLI1—a key effector of the SHH pathway—effectively suppresses the invasive capacity of OKC fibroblasts.

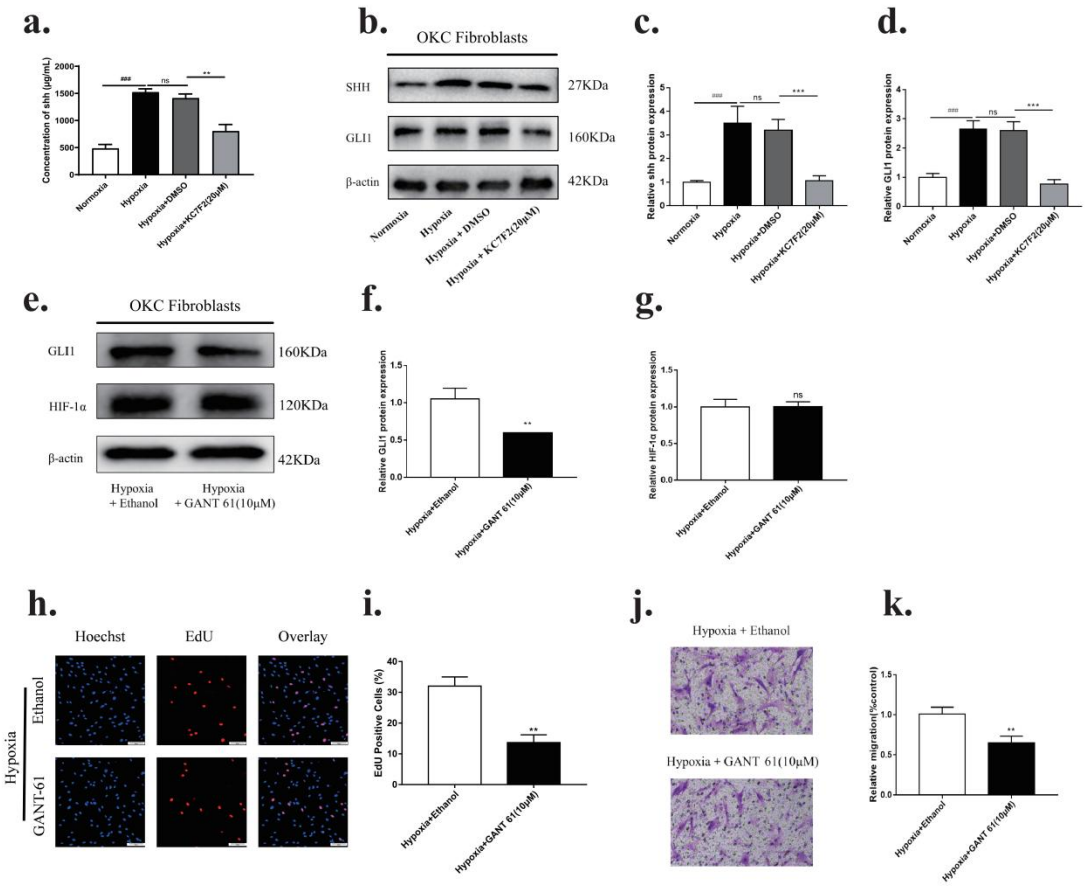


FIGURE 5 (a) Secreted Shh levels in OKC fibroblasts under hypoxic conditions after 24-hour treatment with the HIF-1α inhibitor KC7F2; (b) Protein expression levels of SHH and GLI1 in OKC fibroblasts. (c) Statistical analysis of SHH protein expression; (d) Statistical analysis of GLI1 protein expression; (e) Protein expression levels of GLI1 and HIF-1α in OKC fibroblasts following treatment with a GLI1 inhibitor; (f) Statistical analysis of GLI1 protein expression; (g) Statistical analysis of HIF-1α protein expression; (h) EdU labeling in OKC fibroblasts treated with the GLI1 inhibitor GANT-61 for 24 hours was observed under fluorescence microscopy (i) Quantitative analysis of EdU-positive cell percentage in OKC fibroblasts; (j) Cell invasion through Matrigel-coated chambers in OKC fibroblasts treated with the GLI1 inhibitor GANT-61 for 24 hours;(k) Quantitative analysis of cell invasion percentage through Matrigel-coated chambers in OKC fibroblasts. (n=3, $^{ns}P \geq 0.05$, $^{*}P < 0.05$, $^{**}P < 0.01$, $^{***}P < 0.001$) .

3.7 Hypoxia attenuates the pro-osteogenic effects of OKC fibroblasts.

After 7 days, OKC group (rBMSCs cultured with CM from normoxic OKC fibroblasts) showed higher alkaline phosphatase (ALP) staining and activity than NC group and OM group (cultured without CM or with CM from OM fibroblasts). In contrast, HYPO-OKC group(rBMSCs cultured with CM from hypoxic OKC fibroblasts) exhibited markedly reduced ALP levels compared to those in the OKC group (Figure 6a-c). Quantitative real-time

PCR revealed significant upregulation of osteogenic-related genes (Col1a1, Runx2, Bmp2) in the OKC group versus NC/OM controls, whereas HYPO-OKC group downregulated these genes compared to OKC group (Figure 6d). Western blot further confirmed elevated RUNX2 and BMP4 protein expression in the OKC group versus NC group, which was significantly attenuated under hypoxia (Figure 6e-h). Collectively, normoxic OKC fibroblasts enhance rBMSC osteogenic differentiation, while OKC fibroblasts under hypoxic conditions suppress this capacity.

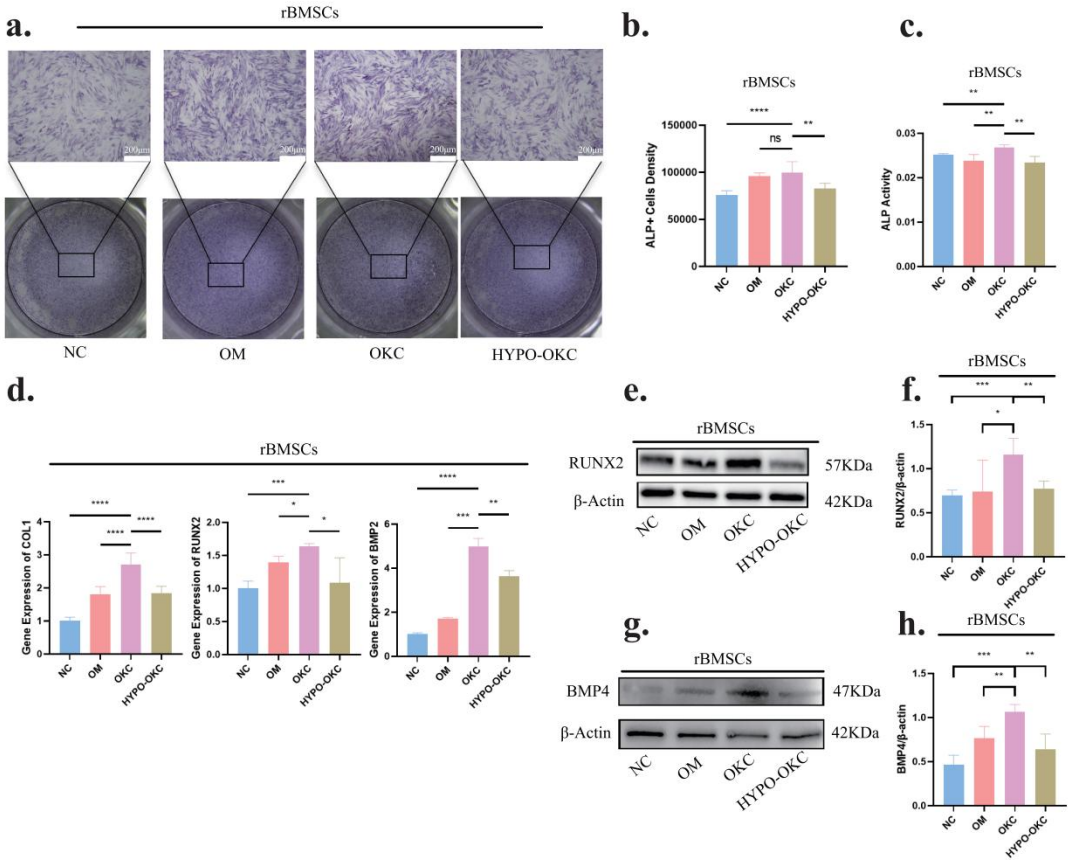


FIGURE 6 (a) Microscopic view of stained rBMSCs (7 days, 4×);(b) Quantitative analysis of ALP staining density; (c)Quantitative analysis of ALP enzymatic activity;(d) Quantitative analysis of osteogenic gene expression in rBMSCs by q-PCR (7 days); (e) RUNX2 protein expression in rBMSCs by Western Blot (7 days); (f) Quantitative analysis of RUNX2 expression; (g) BMP4 protein expression in rBMSCs by Western Blot (7 days); (h) Quantitative analysis of BMP4 expression. (n=3, $^{ns}P \geq 0.05$, $^{*}P<0.05$, $^{**}P<0.01$, $^{***}P < 0.001$)

3.8 Hypoxia enhances the pro-osteoclastic effect of OKC fibroblasts.

Experimental analyses demonstrated enhanced osteoclastic activity in the OKC group versus NC and OM groups. TRAP staining (7 days) revealed significantly increased TRAP-positive multinucleated cells in the OKC group , an effect further amplified in the

HYPO-OKC group (Figure 7a,b). Bone resorption pit assays (10 days) showed larger resorption areas in the OKC group compared to NC/OM controls, with the HYPO-OKC group exhibiting the highest resorption (Figure 7c,d). Western Blot confirmed elevated CTSK and MMP9 protein levels in the OKC group compared to NC/OM controls, with further elevation observed in the HYPO-OKC group (Figure 7e-g).

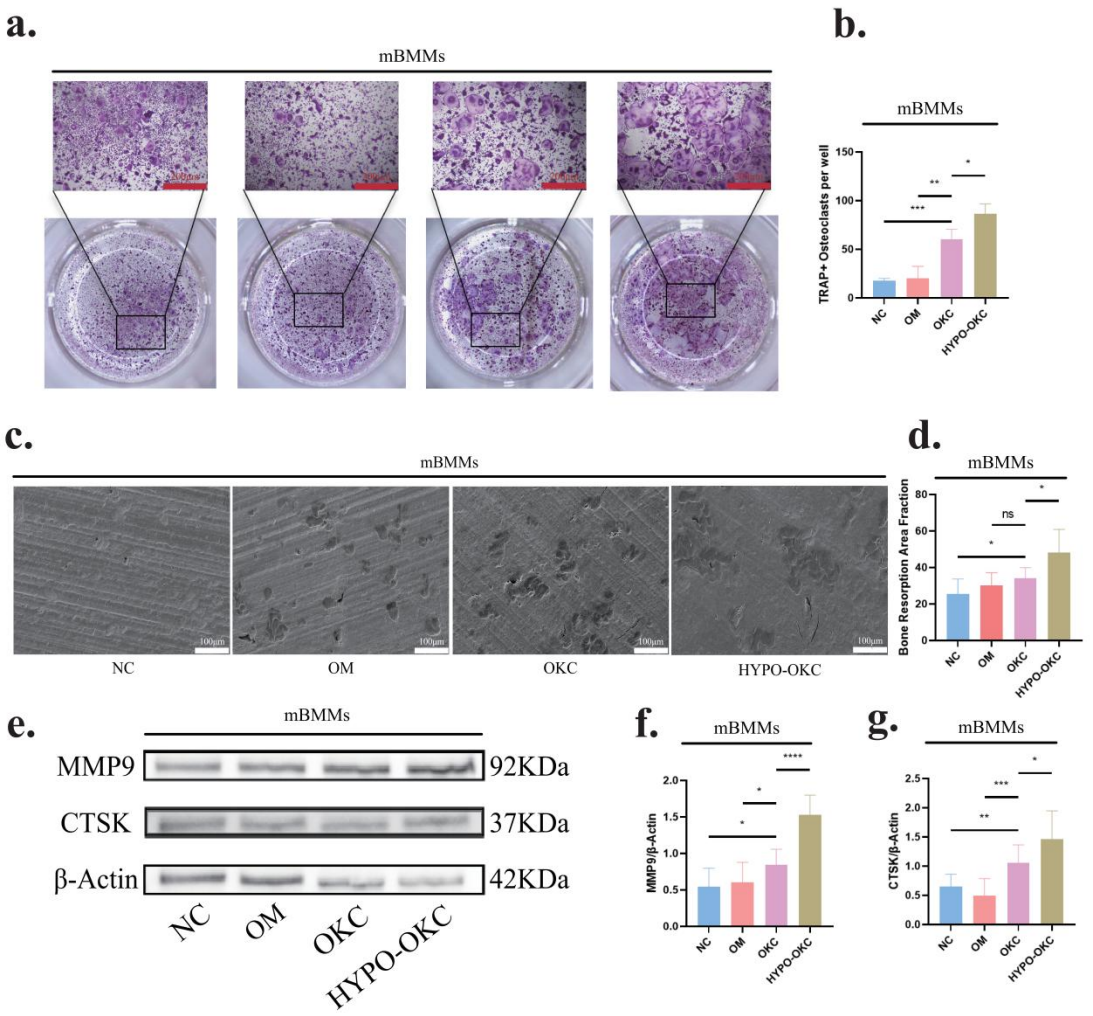


FIGURE 7 (a) TRAP staining of mBMMs (7 days, 10×); (b) Quantitative analysis of TRAP-positive multinucleated cells; (c) Bone resorption pit assay of mBMMs cultured with conditioned medium (10 days, 200×); (d) Quantitative analysis of bone resorption pit area; (e) MMP9 and CTSK protein expression in osteoclast-differentiated mBMMs by Western Blot. (f) Quantitative analysis of MMP9 expression; (g) Quantitative analysis of CTSK expression ..(n=3, $^{ns}P \geq 0.05$, $^{*}P < 0.05$, $^{**}P < 0.01$, $^{***}P < 0.001$)

3.9 Transcriptome sequencing with bioinformatics analysis and detection

Our in vitro experiments demonstrated that hypoxia modulates the paracrine activity of OKC fibroblasts, leading to the suppression of osteogenic differentiation in rBMSCs and the

promotion of osteoclastic differentiation in mBMMs. Since jawbone destruction represents a major clinical manifestation of OKC, we further investigated the molecular mechanisms underlying this bone loss by focusing on the regulatory effects of CM derived from hypoxic OKC fibroblasts on osteoclast precursor cells (mBMMs).

To investigate whether the SHH signaling pathway is activated in mBMMs—we performed transcriptome sequencing, bioinformatic analysis, and Western blot (WB). WB results showed no significant difference in GLI1 protein expression between the OKC group and the HYPO-OKC group (Fig 8a). Consistently, GSEA also revealed no enrichment of the Hedgehog signaling pathway in mBMMs (Fig8 b). Taken together, these data indicate that the SHH pathway is not directly activated within mBMMs themselves under these experimental conditions. Compared to OKC group(mBMMs cultured with CM derived from OKC fibroblasts grown under normoxia), HYPO-OKC group (mBMMs cultured with conditioned medium derived from OKC fibroblasts exposed to hypoxia) exhibited 143 upregulated and 156 downregulated genes (Fig8 c). Among the upregulated differentially expressed genes, PLK1 ranked first. PLK1 (Polo-like kinase 1) is a critical serine/threonine protein kinase belonging to the Polo-like kinase family and plays a vital role in cell cycle regulation, particularly during mitosis[28]. And the expression of other mitosis-related markers such as MCM5, Aurora B, Cyclin A, and Cyclin B was also elevated (Fig8 d). GSEA revealed significant enrichment of the "mitosis" process in the HYPO-OKC group, a finding corroborated by Reactome pathway analysis (Fig8 e), which further showed marked upregulation of key cell cycle regulators—including PLK1, Cyclin A, Cyclin B, Aurora B, CDC25B, and CDC25A—within the "cell cycle" regulatory network. To validate the bioinformatic analysis results, q-PCR was performed. The findings revealed that, compared to the OKC group, the relative mRNA expression levels of mitosis-related markers (PLK1, Cyclin B1, and MCM5) in mBMMs of the HYPO-OKC group were significantly upregulated. Western Blot analysis (7-day culture) revealed that the expression levels of mitosis-related proteins (PLK1, Cyclin B1, and MCM5) in mBMMs were significantly upregulated in the HYPO-OKC group compared to the OKC group.

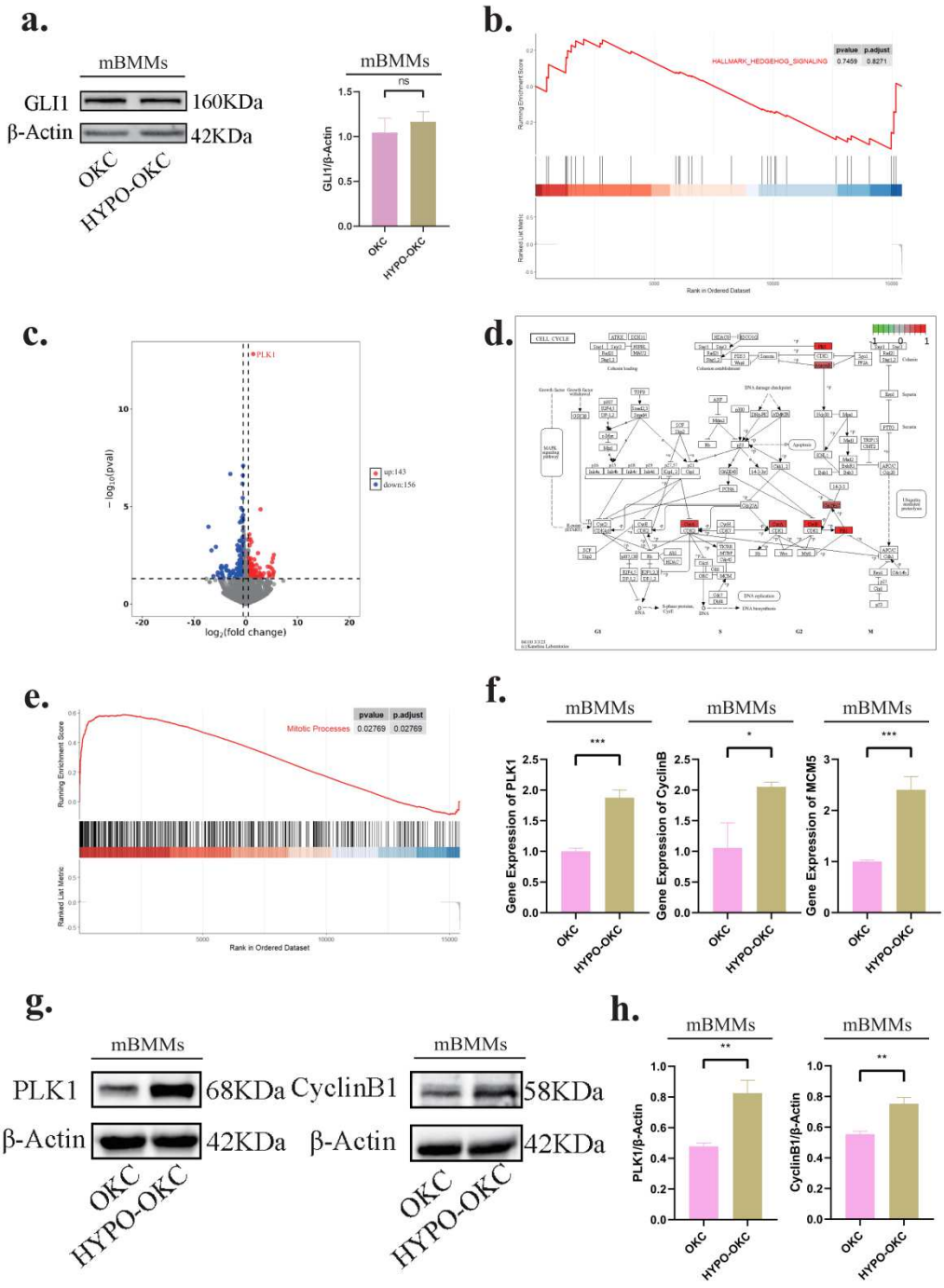


FIGURE 8 (a)GLI1 protein expression and quantitative analysis in mBMMs cultured with CM from hypoxic OKC fibroblasts by Western Blot; (b)GSEA detected the overall enrichment trends of Hedgehog signaling pathway gene sets in HYPO-OKC group; (c)Volcano plot comparing gene expression profiles in mBMMs treated with conditioned medium from the OKC group versus the HYPO-OKC group; (d) Reactome pathway analysis of the "Cell Cycle" regulatory network; (e)GSEA enrichment analysis of the "Mitosis" process;(f)Quantitative analysis of mitosis-related gene expression in rBMSCs by q-PCR (7 days);(g)Mitosis-related markers expression in mBMMs cultured with CM from hypoxic

OKC fibroblasts by Western Blot;(h)Quantitative analysis of mitosis-related markers expression. (n=3, $^{ns}P \geq 0.05$, $^{*}P < 0.05$, $^{**}P < 0.01$, $^{***}P < 0.001$)

3.10 nMS-1286937 reverses the promoting effect of HYPO-OKC conditioned medium on osteoclast differentiation in mBMMs.

Given the central role of PLK1 in cell cycle progression and its significant upregulation identified in our transcriptomic analysis, we hypothesized that PLK1 might mediate the enhanced osteoclastogenic effect induced by hypoxic OKC fibroblast CM. To test this hypothesis, we first determined an appropriate working concentration of the PLK1 inhibitor nMS-1286937 through preliminary screening (see Supplementary 2 Information). Based on these results, a concentration of 0.01 μM nMS-1286937 was used for subsequent functional experiments. Osteoclast differentiation was assessed by TRAP staining after 7 days of culture. The results showed no significant difference in TRAP-positive multinucleated cells between NC group(mBMMs cultured in medium lacking both CM and nMS-1286937) and NC+DMSO group(mBMMs cultured in medium containing the same amount of DMSO vehicle as the inhibitor group). In contrast, HYPO-OKC+DMSO group(mBMMs cultured in medium containing CM from hypoxic OKC fibroblasts and the same amount of DMSO vehicle as the treatment group)exhibited a significant increase in TRAP-positive cells compared to the NC+DMSO group. Importantly, addition of nMS-1286937 (HYPO-OKC+inhibitor group) markedly reduced the number of TRAP-positive multinucleated cells compared to the HYPO-OKC+DMSO group (Fig. 9a, b). Consistent with the phenotypic observation, Western blot analysis after 7-day culture revealed no significant difference in the expression of osteoclast-related proteins (CTSK and MMP9) between the HYPO-OKC and HYPO-OKC+DMSO groups. However, the HYPO-OKC+inhibitor group showed significant downregulation of both CTSK and MMP9 compared to the HYPO-OKC+DMSO group (Fig. 9c, d).

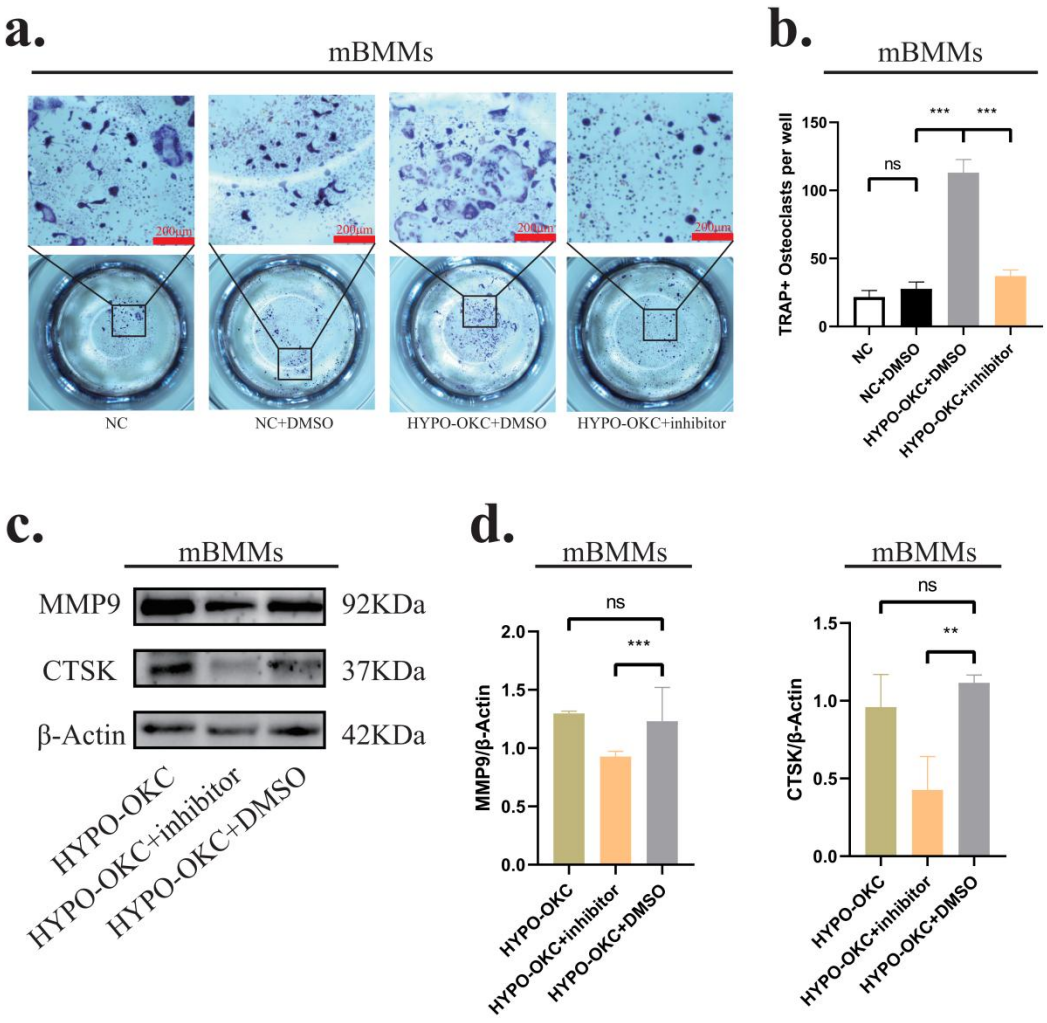


FIGURE 9 (a) TRAP staining of mBMMs (7 days, 10×); (b) Quantitative analysis of TRAP-positive multinucleated cells; (c) MMP9 and CTSK protein expression in osteoclast-differentiated mBMMs by Western Blot. (d) Quantitative analysis of MMP9 and CTSK expression (n=3, $^{ns}P \geq 0.05$, $^{*}P < 0.05$, $^{**}P < 0.01$, $^{***}P < 0.001$) .

Discussion

Histologically, OKC consists of a lining epithelium and a fibrous connective tissue capsule wall. The lining epithelium has long been a focal point of OKC research[29]. However, primary OKC epithelial cells exhibit extremely slow growth and are prone to senescence upon passaging[30]. In 1975, the team led by Browne RM first demonstrated that fibroblasts within the fibrous connective tissue capsule wall play a crucial role in the biological behavior of OKC[31]. Recent studies have further revealed that OKC fibroblasts are key constituents of the microenvironment, which can promote OKC proliferation,

invasion, and osteoclastogenesis through interactions with epithelial cells[32,33,34]. Our bioinformatic analyses of OKC transcriptomic and single-cell data further confirm that OKC fibroblasts play a significant role in hypoxia response, proliferation, invasion, and bone remodeling activities. Therefore, this study was designed to focus specifically on the OKC stromal compartment.

Previous studies have indicated the presence of hypoxia in the OKC microenvironment, although relevant research remains relatively limited[35,30,36]HIF-1α, a key transcription factor induced by hypoxia, plays an important role in tumor development and progression. Prior studies have demonstrated that regulating HIF-1α expression significantly affects tumor cell migration, invasion, and bone remodeling capabilities in colorectal cancer, ovarian cancer, hepatocellular carcinoma, and odontogenic tumors[37,38,39,40,41], suggesting that hypoxia-dependent HIF-1α signaling plays a crucial role in tumor-related biological behaviors. In this study, immunohistochemistry was employed to detect HIF-1α expression in OKC lesion tissues. The results showed that HIF-1α expression was significantly elevated in both the epithelium and stroma of OKC compared to dentigerous cysts (DC) and oral mucosa (OM), further confirming the presence of a hypoxic microenvironment within OKC tissues, which is consistent with the observations by Yanping Zou[36]. However, differing from the previous report by Malu Miranda da Costa[35]. This study found that HIF-1α was expressed throughout the entire epithelial layer of OKC, with stronger expression in the basal layer, rather than being limited to the superficial epithelium adjacent to the cystic lumen. Furthermore, high expression of GLI1, Ki-67, and MMP-9 was observed in the OKC stroma, and Spearman's rank correlation analysis revealed positive correlations between HIF-1α and the expression of GLI1, Ki-67, and MMP-9. These findings indicate that hypoxia-driven HIF-1α may play an important role in the development of OKC mediated by stromal fibroblasts.

Therefore, a physical hypoxia model(hypoxic chamber) was further employed to simulate in vivo hypoxic conditions[42] and found that hypoxia-induced HIF-1α activates the SHH signaling pathway in OKC fibroblasts. Treatment with the HIF-1α inhibitor KC7F2 effectively suppressed the activation of this pathway, whereas inhibition of GLI1 using GANT61 similarly reduced SHH signaling activity without affecting HIF-1α expression levels. These findings indicate that in OKC fibroblasts, hypoxia-mediated HIF-1α acts upstream of the SHH signaling pathway and positively regulates its activity. Further functional assays showed that under hypoxic conditions, inhibition of GLI1 with GANT61 significantly decreased both the proliferative and invasive capacities of OKC fibroblasts. This suggests that blocking the SHH signaling pathway can effectively attenuate the malignant phenotypic driven by hypoxia and HIF-1α. In summary, this set of experiments demonstrates that hypoxia activates the SHH signaling pathway via upregulation of HIF-1α, thereby

promoting the proliferation and invasion of OKC fibroblasts.

In osteogenic and osteoclast differentiation assays, we employed rat bone marrow mesenchymal stem cells (rBMSCs) and mouse bone marrow mononuclear macrophages (mBMMs) to assess the impact of OKC fibroblast-conditioned medium on bone remodeling. Conditioned medium (CM) derived from OKC fibroblasts under normoxia (OKC group) exhibited a "dual-activation" effect via paracrine signaling, promoting both osteogenic differentiation of rBMSCs and osteoclast differentiation of mBMMs under standard culture conditions. In contrast, CM collected from OKC fibroblasts after hypoxia treatment (HYPO-OKC, 1% O_2, 24 h) altered this regulation: osteogenic capacity was suppressed while pro-osteoclastic activity was further enhanced. The hypoxia-driven shift toward “inhibited osteogenesis and enhanced osteoclastogenesis” disrupts bone homeostasis, promoting net bone resorption and providing a mechanistic basis for the jawbone destruction seen in OKC though the specific molecular pathways require further investigation.

Subsequently, we focused on characterizing the altered secretome profile (HYPO-OKC group) and identifying downstream effectors in the target cells, which led us to PLK1. Interestingly, differential gene expression analysis indicated that PLK1 was significantly upregulated in the hypoxia group (Fig. 8c) while the SHH pathway is not directly activated in osteoclast precursor cells under the influence of hypoxic OKC fibroblasts. Moreover, both GSEA and Reactome pathway analyses suggested significant enrichment of the "mitosis" process. PLK1, as a key kinase regulating the cell cycle (particularly mitosis), is closely associated with the proliferation and differentiation of osteoclast precursors. Subsequent experiments confirmed that the PLK1 inhibitor nMS-1286937 could significantly reverse the promoting effect of hypoxic conditioned medium on osteoclast differentiation in mBMMs (Fig. 9). Based on these results, we propose that PLK1 may be a critical downstream target regulating OKC-related bone resorption in the hypoxic microenvironment. This offers a new potential direction for targeted intervention in OKC-associated bone destruction.

Several limitations exist in this study. First, at the molecular level, although HIF-1α regulates the SHH pathway, whether a direct transcriptional regulatory relationship exists between them remains unclear. Second, at the intercellular communication level, while phenotypic changes in bone remodeling induced by fibroblast paracrine signaling under hypoxic conditions have been identified, the key signaling molecules and regulatory networks involved have not yet been resolved. Future studies combining secretome analysis with functional validation may systematically elucidate the molecular basis underlying the “inhibited osteogenesis–promoted osteoclastogenesis” phenotypic shift, thereby providing new clues for understanding the pathological mechanisms of OKC.

Conclusion

The biological mechanisms underlying the progression of OKC remain incompletely understood. This study elucidates the mechanisms by which hypoxia drives OKC progression (Figure 10): Hypoxia-induced HIF-1α promotes the proliferation and invasion of OKC fibroblasts by activating the SHH signaling pathway. Concurrently, OKC fibroblasts under hypoxic conditions stimulate osteoclasts to secrete increased levels of PLK1, leading to bone resorption. Therefore, targeting the HIF-1α-SHH axis and/or PLK1 may represent a potential therapeutic strategy for OKC.

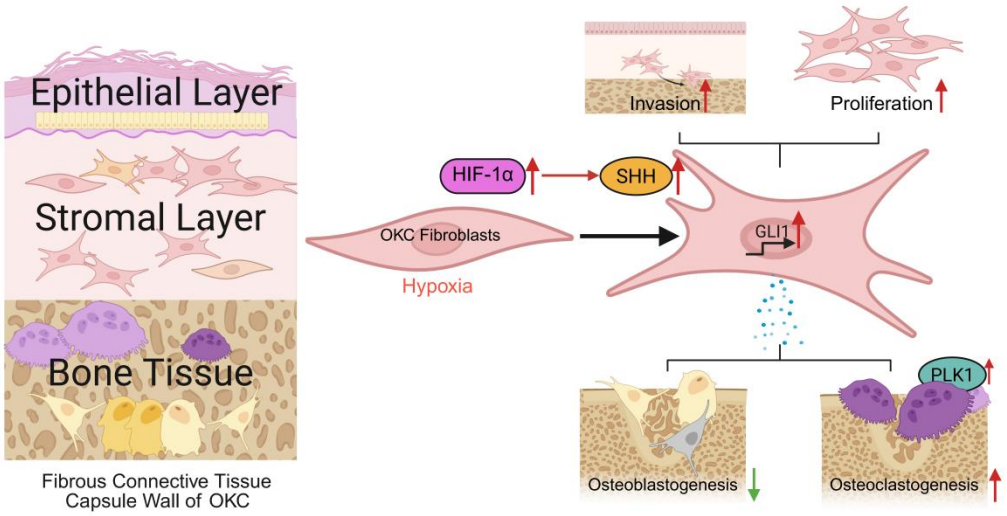


FIGURE10 Hypoxia in the OKC microenvironment upregulates HIF-1α expression in fibroblasts. HIF-1α activates the SHH/GLI1 pathway to promote fibroblast proliferation and invasion. Hypoxic fibroblasts enhance osteoclast differentiation by upregulating PLK1 expression in osteoclast precursor cells via paracrine signaling, while suppressing the osteogenic differentiation of osteogenic precursor cells, leading to bone homeostasis imbalance.

Acknowledgements

This work was supported by the National Natural Science Foundation of China (Grant No. 82560195) and the Yunnan Provincial Reserve Talents Program for Young and Middle-aged Academic and Technical Leaders (Grant No. 202305AC160001).

Human Ethics Approval

Ethical approval for the human subject involved in this case report was obtained from the Medical Ethics Committee of the Affiliated Stomatological Hospital of Kunming Medical University (Approval Nos. KYKQ2022MEC0074 and

KYKQ2024MEC0055). Informed consent was obtained from the patient and/or their legal guardian(s).

Animal Ethics Approval

Ethical approval for the animal study was obtained from the Experimental Animal Welfare Ethics Committee of Kunming Medical University (Approval No. KMMUD2025028). The parts of this study involving human participants were carried out in accordance with the Declaration of Helsinki and relevant guidelines and regulations. All methods were carried out in accordance with relevant guidelines and regulations.

References

1. Gorlin, R. J. Nevoid basal cell carcinoma (Gorlin) syndrome. *Genetics in Medicine* **6**, 530–539 (2004).

2. Bresler, S. C., Padwa, B. L. & Granter, S. R. Nevoid Basal Cell Carcinoma Syndrome (Gorlin Syndrome). *Head and Neck Pathol* **10**, 119–124 (2016).

3. Chen, P., Liu, B., Wei, B. & Yu, S. The clinicopathological features and treatments of odontogenic keratocysts.

4. Wright, J. M. & Vered, M. Update from the 4th Edition of the World Health Organization Classification of Head and Neck Tumours: Odontogenic and Maxillofacial Bone Tumors. *Head and Neck Pathol* **11**, 68–77 (2017).

5. Li, T.-J. The Odontogenic Keratocyst: A Cyst, or a Cystic Neoplasm? *J Dent Res* **90**, 133–142 (2011).

6. Stoelinga, P. J. W. Keratocystic odontogenic tumour (KCOT) has again been renamed odontogenic keratocyst (OKC). *International Journal of Oral and Maxillofacial Surgery* **48**, 415–416 (2019).

7. Al-Moraissi, E. A., Kaur, A., Gomez, R. S. & Ellis, E. Effectiveness of different treatments for odontogenic keratocyst: a network meta-analysis. *International Journal of Oral and Maxillofacial Surgery* **52**, 32–43 (2023).

8. Lin, H., Zhong, X., Zhou, N. & Huang, X.-P. Mandibular reconstruction after excision of recurrent odontogenic keratocyst using a novel mandibular distraction osteogenesis method–a case report. *Head Face Med* **19**, 21 (2023).

9. Babar, Q., Saeed, A., Tabish, T. A., Sarwar, M. & Thorat, N. D. Targeting the tumor microenvironment: Potential strategy for cancer therapeutics. *Biochimica et Biophysica Acta (BBA) - Molecular Basis of Disease* **1869**, 166746 (2023).

10. Hartupee, C. *et al.* Pancreatic cancer tumor microenvironment is a major therapeutic barrier and target. *Front. Immunol.* **15**, 1287459 (2024).

11. Wang, L. *et al.* Advances in targeting tumor microenvironment for immunotherapy. *Front. Immunol.* **15**, 1472772 (2024).

12. Mortezaee, K. & Majidpoor, J. The impact of hypoxia on extracellular vesicle secretome profile of cancer. *Med Oncol* **40**, 128 (2023).

13. Yu, Y. *et al.* Hypoxia upregulates the expression of PD-L1 via NPM1 in breast cancer. *J Immunother Cancer* **13**, e010151 (2025).

14. Zhang, T.-Q., Lv, Q.-Y. & Jin, W.-L. The cellular-centered view of hypoxia tumor microenvironment: Molecular mechanisms and therapeutic interventions. *Biochimica et Biophysica Acta (BBA) - Reviews on Cancer* **1879**, 189137 (2024).

15. Bae, T., Hallis, S. P. & Kwak, M.-K. Hypoxia, oxidative stress, and the interplay of HIFs and NRF2 signaling in cancer. *Exp Mol Med* **56**, 501–514 (2024).

16. Nakayama, K. & Kataoka, N. Regulation of Gene Expression under Hypoxic Conditions. *IJMS* **20**, 3278 (2019).

17. Chen, W. *et al.* HIF-1α Regulates Bone Homeostasis and Angiogenesis, Participating in the Occurrence of Bone Metabolic Diseases. *Cells* **11**, 3552 (2022).

18. De Heer, E. C., Jalving, M. & Harris, A. L. HIFs, angiogenesis, and metabolism: elusive enemies in breast cancer. *Journal of Clinical Investigation* **130**, 5074–5087 (2020).

19. Jing, X. *et al.* Role of hypoxia in cancer therapy by regulating the tumor microenvironment. *Mol Cancer* **18**, 157 (2019).

20. Kim, L. C. & Simon, M. C. Hypoxia-Inducible Factors in Cancer. *Cancer Research* **82**, 195–196 (2022).

21. Li, Y., Zhao, L. & Li, X.-F. Hypoxia and the Tumor Microenvironment. *Technol Cancer Res Treat* **20**, 15330338211036304 (2021).

22. Tao, J. *et al.* Spatiotemporal correlation between HIF -1α and bone regeneration. *The FASEB Journal* **36**, e22520 (2022).

23. Pan, S. & Li, T.-J. PTCH1 mutations in odontogenic keratocysts: Are they related to epithelial cell proliferation? *Oral Oncology* **45**, 861–865 (2009).

24. Qu, J. et al. GDC-0449 suppresses odontogenic keratocyst aggressiveness in fibroblasts by upregulating SPARC via Hedgehog pathway inhibition. Archives of oral biology 179, 106374 (2025).

25. Qu, J. *et al.* Underestimated PTCH1 mutation rate in sporadic keratocystic odontogenic tumors. *Oral Oncology* **51**, 40–45 (2015).

26. Wei, M. *et al.* Oroxylin A increases the sensitivity of temozolomide on glioma cells by hypoxia-inducible factor 1α/hedgehog pathway under hypoxia. *Journal Cellular Physiology* **234**, 17392–17404 (2019).

27. Lei, J. *et al.* Hedgehog signaling regulates hypoxia induced epithelial to mesenchymal transition and invasion in pancreatic cancer cells via a ligand-independent manner. *Mol Cancer* **12**, 66 (2013).

28. Zhang, Z. *et al.* Targeting Plk1 Sensitizes Pancreatic Cancer to Immune Checkpoint Therapy. *Cancer Research* **82**, 3532–3548 (2022).

29. Li, T. -J., Browne, R. M. & Matthews, J. B. Quantification of $PCNA^{+}$ cells within odontogenic jaw cyst epithelium. *J Oral Pathology Medicine* **23**, 184–189 (1994).

30. Zhong, W.-Q. *et al.* Elevated ATF4 Expression in Odontogenic Keratocysts Epithelia: Potential Involvement in Tissue Hypoxia and Stromal M2 Macrophage Infiltration. *J Histochem Cytochem.* **67**, 801–812 (2019).

31. Browne, R. M. The pathogenesis of odontogenic cysts: a review. *J Oral Pathology Medicine* **4**, 31–46 (1975).

32. Hong, Y.-Y., Yu, F.-Y., Qu, J.-F., Chen, F. & Li, T.-J. Fibroblasts Regulate Variable Aggressiveness of Syndromic Keratocystic and Non-syndromic Odontogenic Tumors. *J Dent Res* **93**, 904–910 (2014).

33. Man, Q., Li, R., Liu, J., Zhao, Y. & Liu, B. Single-cell analysis reveals immune cellular components in odontogenic keratocysts. *Oral Diseases* **29**, 3420–3432 (2023).

34. Wang, H. & Li, T. The growth and osteoclastogenic effects of fibroblasts isolated from keratocystic odontogenic tumor. *Oral Diseases* **19**, 162–168 (2013).

35. Miranda Da Costa, N. M. *et al.* HIF-1α is Overexpressed in Odontogenic Keratocyst Suggesting Activation of HIF-1α and NOTCH1 Signaling Pathways. *Cells* **8**, 731 (2019).

36. Zou, Y., Wang, R., Zhao, J., Cai, Y. & Zhong, W. Increased M2 Isoform of Pyruvate Kinase in Fibroblasts Contributes to the Growth, Aggressiveness, and Osteoclastogenesis of Odontogenic Keratocysts. *The American Journal of Pathology* **191**, 857–871 (2021).

37. Joshi, H. P. *et al.* Dynamin 2 along with microRNA-199a reciprocally regulate hypoxia-inducible factors and ovarian cancer metastasis. *Proc. Natl. Acad. Sci. U.S.A.* **111**, 5331–5336 (2014).

38. Malard, F. *et al*. Multiple myeloma. *Nature reviews Disease primers* 10, 45 （2024）.

39. Motta, F., Barone, E., Sica, A. & Selmi, C. Inflammaging and Osteoarthritis. *Clinic Rev Allerg Immunol* **64**, 222–238 (2022).

40. Roodman, G. D. Regulation of Osteoclast Differentiation. *Annals of the New York Academy of Sciences* **1068**, 100–109 (2006).

41. Tang, Y.-A. *et al.* Hypoxic tumor microenvironment activates GLI2 via HIF-1α and TGF-β2 to promote chemoresistance in colorectal cancer. *Proc. Natl. Acad. Sci. U.S.A.* **115**, (2018).

42. Janbandhu, V. *et al.* Hif-1a suppresses ROS-induced proliferation of cardiac fibroblasts following myocardial infarction. *Cell Stem Cell* **29**, 281-297.e12 (2022).

Supplementary Files

This is a list of supplementary files associated with this preprint. Click to download.

- Supplementary1.zip
- Supplementary2.pdf